REPORT DOCUMENTATION PAGE

Form Approved OMB NO. 0704-0188

1. REPORT DATE (DD-MM-YYYY)	2. REPORT TYPE	3. DATES COVERED (From - To)
08-11-2013	Final Report	1-Aug-2010 - 31-Jul-2013

4. TITLE AND SUBTITLE
Transport of multivalent electrolyte mixtures in micro- and nanochannels

5a. CONTRACT NUMBER
W911NF-10-1-0290

5b. GRANT NUMBER

5c. PROGRAM ELEMENT NUMBER
611102

6. AUTHORS
A. T. Conlisk, Minami Yoda

5d. PROJECT NUMBER

5e. TASK NUMBER

5f. WORK UNIT NUMBER

7. PERFORMING ORGANIZATION NAMES AND ADDRESSES
Ohio State University Research Foundation
Office of Sponsored Programs
1960 Kenny Rd.
Columbus, OH 43210 -1063

8. PERFORMING ORGANIZATION REPORT NUMBER

9. SPONSORING/MONITORING AGENCY NAME(S) AND ADDRESS (ES)
U.S. Army Research Office
P.O. Box 12211
Research Triangle Park, NC 27709-2211

10. SPONSOR/MONITOR'S ACRONYM(S)
ARO

11. SPONSOR/MONITOR'S REPORT NUMBER(S)
55734-EG.15

12. DISTRIBUTION AVAILIBILITY STATEMENT
Approved for Public Release; Distribution Unlimited

13. SUPPLEMENTARY NOTES
The views, opinions and/or findings contained in this report are those of the author(s) and should not contrued as an official Department of the Army position, policy or decision, unless so designated by other documentation.

14. ABSTRACT
The major goal of this research is to understand charged biomolecules in a biofluid flowing through a micro- or nanochannel interact with a charged surface in the presence of an applied electric field parallel to the wall. In the third and final year of this work, the experimental effort at Georgia Tech has focused on studying the dynamics of colloidal particles, as a model of large charged biomolecules, in combined electroosmotic and Poiseuille flow through microchannels, i.e., in the presence of an applied electric field parallel to the wall and flow shear. The research group at Ohio State has provided theoretical and computational expertise in predicting particle trajectories

15. SUBJECT TERMS
electroosmotic flow, multivalent ions, colloidal particles, particle distribution

16. SECURITY CLASSIFICATION OF:			17. LIMITATION OF ABSTRACT	15. NUMBER OF PAGES	19a. NAME OF RESPONSIBLE PERSON
a. REPORT	b. ABSTRACT	c. THIS PAGE			Albert Conlisk
UU	UU	UU	UU		19b. TELEPHONE NUMBER 614-292-0808

Report Title

Transport of multivalent electrolyte mixtures in micro- and nanochannels

ABSTRACT

The major goal of this research is to understand charged biomolecules in a biofluid flowing through a micro- or nanochannel interact with a charged surface in the presence of an applied electric field parallel to the wall. In the third and final year of this work, the experimental effort at Georgia Tech has focused on studying the dynamics of colloidal particles, as a model of large charged biomolecules, in combined electroosmotic and Poiseuille flow through microchannels, i.e., in the presence of an applied electric field parallel to the wall and flow shear. The research group at Ohio State has provided theoretical and computational expertise in predicting particle trajectories, estimating forces on particles, and predicting particle distribution all for the parameters of the experiments.

Enter List of papers submitted or published that acknowledge ARO support from the start of the project to the date of this printing. List the papers, including journal references, in the following categories:

(a) Papers published in peer-reviewed journals (N/A for none)

Received		Paper
06/25/2012	8.00	Harvey A. Zambrano, Marie Pinti, A. T. Conlisk, Shaurya Prakash. Electrokinetic transport in a water–chloride nanofilm in contact with a silica surface with discontinuous charged patches, Microfluidics and Nanofluidics, (05 2012): 0. doi: 10.1007/s10404-012-0992-9
08/02/2013	9.00	Necmettin Cevheri, Minami Yoda. Evanescent-wave particle velocimetry measurements of zeta-potentials in fused-silica microchannels, ELECTROPHORESIS, (07 2013): 0. doi: 10.1002/elps.201300083
08/19/2011	2.00	Yutaka Kazoe, Minami Yoda. Experimental Study of the Effect of External Electric Fields on Interfacial Dynamics of Colloidal Particles, Langmuir, (08 2011): 0. doi: 10.1021/la202056b
TOTAL:	**3**	

Number of Papers published in peer-reviewed journals:

(b) Papers published in non-peer-reviewed journals (N/A for none)

Received		Paper
TOTAL:		

Number of Papers published in non peer-reviewed journals:

(c) Presentations

Number of Presentations: 0.00

Non Peer-Reviewed Conference Proceeding publications (other than abstracts):

Received		Paper
06/06/2012	7.00	Necmettin Cevheri, Minami Yoda. The effect of divalent counterions on particle velocimetry studies of electrokinetically driven flows, 16th International Symposium on Applications of Laser Techniques to Fluid Mechanics. 09-JUL-12, . : ,
08/02/2013	10.00	Necmettin Cevheri, Minami Yoda. Evanescent-wave particle velocimetry studies of combined electroosmotic and Poiseuille flow, 10th International Symposium on Particle Image Velocimetry (PIV13). 01-JUL-13, . : ,
08/22/2011	1.00	A. T. Conlisk, Minami Yoda. Verification and Validation at the Micro and Nanoscale, AIAA Computational Fluid Dynamics Conference. 28-JUN-11, . : ,
08/23/2011	3.00	A. T. Conlisk, Harvey Zambrano, Haifeng Li, Yutaka Kazoe, Minami Yoda. Particle-wall interactions in micro/nanochannels, 50th AIAA Aerospace Sciences Conference . 09-JAN-12, . : ,
10/22/2013	11.00	Harvey Zambrano, A. T. Conlisk. Controlling the electroosmotic transport in nanochannels: effect of divalent counter-ions, AIAA Aerospace Sciences Meeting. 07-JAN-13, . : ,
TOTAL:	**5**	

Number of Non Peer-Reviewed Conference Proceeding publications (other than abstracts):

Peer-Reviewed Conference Proceeding publications (other than abstracts):

Received		Paper
04/13/2012	4.00	. A Theoretical Study of Biological Cell/ColloidalParticle Transport in Microchannels, AIAA Aerospace Sciences Meeting. 06-JAN-12, . : ,
04/13/2012	5.00	A. T. Conlisk, Harvey Zambrano, Haifeng Li, Yutaka Kazoe, Minami Yoda . Particle-wall interactions in micro/nanochannels, AIAA Aerospace Sciences Meeting. 06-JAN-12, . : ,
06/06/2012	6.00	Necmettin Cevheri, Minami Yoda. Evanescent-wave particle velocimetry studies of electrokinetically driven flows: Divalent counterion effects, 2012 3rd Micro/Nanoscale Heat & Mass Transfer International Conference (MNHMT2012). 03-MAR-12, . : ,
TOTAL:	**3**	

Number of Peer-Reviewed Conference Proceeding publications (other than abstracts):

(d) Manuscripts

Received	Paper

TOTAL:

Number of Manuscripts:

Books

Received	Paper

TOTAL:

Patents Submitted

Patents Awarded

Awards

Graduate Students

NAME	PERCENT_SUPPORTED
FTE Equivalent:	
Total Number:	

Names of Post Doctorates

NAME	PERCENT_SUPPORTED
Harvey Zambrano	0.75
FTE Equivalent:	**0.75**
Total Number:	**1**

Names of Faculty Supported

NAME	PERCENT_SUPPORTED

FTE Equivalent:
Total Number:

Names of Under Graduate students supported

NAME	PERCENT_SUPPORTED

FTE Equivalent:
Total Number:

Student Metrics

This section only applies to graduating undergraduates supported by this agreement in this reporting period

The number of undergraduates funded by this agreement who graduated during this period: .....
The number of undergraduates funded by this agreement who graduated during this period with a degree in science, mathematics, engineering, or technology fields:.....
The number of undergraduates funded by your agreement who graduated during this period and will continue to pursue a graduate or Ph.D. degree in science, mathematics, engineering, or technology fields:.....
Number of graduating undergraduates who achieved a 3.5 GPA to 4.0 (4.0 max scale):.....
Number of graduating undergraduates funded by a DoD funded Center of Excellence grant for Education, Research and Engineering:.....
The number of undergraduates funded by your agreement who graduated during this period and intend to work for the Department of Defense .....
The number of undergraduates funded by your agreement who graduated during this period and will receive scholarships or fellowships for further studies in science, mathematics, engineering or technology fields: .....

Names of Personnel receiving masters degrees

NAME

Total Number:

Names of personnel receiving PHDs

NAME

Total Number:

Names of other research staff

NAME	PERCENT_SUPPORTED

FTE Equivalent:
Total Number:

Sub Contractors (DD882)

Inventions (DD882)

Scientific Progress

Technology Transfer

Introduction

Microfluidics, defined here as the study of flows with overall dimensions ranging from a few μm to a few hundred μm, has been a major area of research over the last decade [1; 2]. Diffusion, which occurs over time scales proportional to the square of the length scale, becomes much faster for flows at such small length scales, and many of the applications of microfluidics exploit this rapid diffusion. Microfluidic devices such as "Labs on a Chip" (LOC) and micro-total analysis systems (μTAS) are used for high-throughput biomolecular and cellular separation, reaction and detection, among other applications

A major enabling technology for LOC is controlling the (usually incompressible, low Reynolds number, and internal) flows flow of "biofluids"—aqueous solutions containing electrolytes and charged biomolecules—through nano- and microchannels. The surface of the walls of such channels will become charged when exposed to biofluids, and this (usually negatively) charged surface will be screened in turn by a thin layer of counterions (usually cations) drawn from the biofluid. This screening layer is known as the electric double layer (EDL), and it has a charge distribution characterized by the wall zeta-potential ζ_w [3]. The overall thickness of the EDL is about five times the Debye screening length λ_D (the $1/e$ lengthscale for the potential from the solution of the linearized Poisson-Boltzmann equation), which varies from a few Ångstroms for aqueous electrolyte solutions at molar concentrations of $O(1$ mol/L) to a few microns for very pure water with a resistivity of 10 MΩ·cm.

In the electroomostic (EO) flows commonly used in LOC, a voltage gradient, or external electric field of magnitude E, is applied parallel to the wall to drive the charged fluid in the EDL, and the uniform flow of neutral bulk fluid is driven by viscous effects by the nonuniform "boundary layer-like" flow of fluid molecules and counterions in the EDL. Many LOC applications employ EO flow because this uniform flow in the bulk gives higher flow rates and less convective dispersion than the parabolic velocity profile (with the same maximum velocity) of pressure-driven Poiseuille flow.

Research Accomplishments and Army Relevance

The major goal of this research is to understand charged biomolecules in a biofluid flowing through a micro- or nanochannel interact with a charged surface in the presence of an applied electric field parallel to the wall. In the third and final year of this work, the experimental effort at Georgia Tech led by Dr. Yoda has focused on studying the dynamics of colloidal particles, as a model of large charged biomolecules, in combined electroosmotic and Poiseuille flow through microchannels, *i.e.*, in the presence of an applied electric field parallel to the wall and flow shear. The objectives for the experimental effort are to:

1) Determine how the nonlinear electrokinetic repulsive lift force reported by Kazoe and Yoda [4] is affected by flow shear;

2) Verify our hypothesis that tracer particles of different sizes in this nonuniform flow with an electric field parallel to the wall will have different average wall-normal distances, and hence sample different average particle velocities, in this shear flow.

The objectives of the theoretical and computational effort at the Ohio State University led by Dr. Conlisk are to:

1) Calculate the velocity of a colloidal particle as it moves near a wall;
2) Predict the number density of a population of colloidal particles near the wall of a channel;
3) Determine the origin, nature and magnitude of the forces on the types of colloidal particles used in the experiments in the presence of shear;
4) Determine using molecular simulations, the effect that different divalent cations have on electroosmotic flow.

Experimental Results and Research Accomplishments

The experimental effort uses evanescent-wave particle tracking velocimetry (PTV), which estimates velocity fields from the displacements of colloidal fluorescent polystyrene (PS) particles of radius $a \leq 0.5$ μm over two successive exposures separated by a time interval Δt. The particles, which are (nearly) density-matched to the fluid, are illuminated by evanescent waves generated by the total internal reflection (TIR) of light at the refractive-index interface between the fluid, an aqueous monovalent electrolyte solution, and the fused-silica wall of the microchannel. The method has been used by various researchers, including Dr. Yoda, to study microchannel flows over the first ~0.5 μm next to the wall [5–8]. Although the method is inherently limited to near-wall flows, the spatial resolution of evanescent-wave particle velocimetry is significantly better than the leading velocimetry method for microchannels, micro-particle image velocimetry (μPIV), with its typical minimum depth of correlation of 2 μm [9].

In most PTV applications, the fluid velocity is assumed to be identical to the particle velocity. In EO flow, however, the particle velocity is <u>not</u> that of the fluid because the surface of the particles (like the walls of the channel) also become charged in the presence of an aqueous electrolyte solution. This particle surface charge is characterized by the particle zeta-potential ζ_p, which, much like the wall zeta-potential ζ_w. is the electric potential a counterion diameter away from the surface of the particle. The external electric field that drives the flow will therefore also transport the particle tracers. For particle tracers with a (usually negative) surface charge (to minimize particle deposition upon the negatively charged

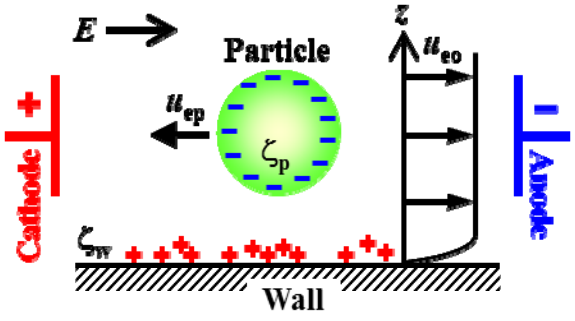

Figure 1 A negatively charged particle near a negatively charged wall. Note that only the mobile cations are shown near the wall.

wall), E will drive the tracers towards the cathode, a phenomenon known as electrophoresis [3]. A tracer particle will therefore be convected by EO flow and driven by electrophoresis in opposite directions (Fig. 1). The actual velocity of the particle u_p will therefore be the superposition of the EO flow velocity u_{eo} and the particle's electrophoretic velocity u_{ep}, which for the case of "thin" EDLs (where $\lambda_D / a \ll 1$ and a is the particle radius) is:

$$u_p = u_{ep} + u_{eo} = \frac{\varepsilon}{\mu}(\zeta_p - \zeta_w) E \tag{1}$$

where ε and μ are the permittivity and dynamic viscosity of the fluid, respectively. So the particle velocity will only be equal to the fluid velocity in EO flow for $\zeta_p = 0$.

These particles are also subject to forces along the cross-stream direction, specifically normal to the wall. It has been known for almost 30 years that $a \approx 2.5$ μm–5 μm particles convected by a simple shear flow, as is the case for Poiseuille flow driven by a pressure gradient very close to the wall, experience a repulsive force, known as "shear-induced electrokinetic lift," due to electroviscous effects [10]. Dr. Yoda's group has also shown that smaller $a \approx 0.2$ μm–0.5 μm particles convected by a uniform flow in the presence of an electric field parallel to the wall, as is the case for EO flow driven by a voltage gradient, also experience a repulsive force, with a magnitude that appears, admittedly over a limited range of parameters, to be proportional to E^2 and a^2, in agreement with theoretical predictions of a"dielectrophoretic-like" repulsive force due to nonuniformities in the local electric field in gap between the particle and wall [11]. However, the discrepancy between theoretical predictions and experimental estimates of the magnitudes of both the dielectrophoretic-like repulsion and shear-induced electrokinetic lift [12] are at least an order of magnitude, suggesting that we lack a theoretical understanding of both types of wall-normal forces.

Given that microchannel flows are most commonly driven by voltage and pressure gradients, these results suggest that the dynamics of tracer particles within 1 μm of the wall are quite complicated, and these dynamics must be accounted for to obtain accurately "map" particle velocities to flow velocities in LOC. Improving our understanding of these dynamics is therefore critical in improving the performance of LOC given that particle velocimetry techniques are the leading technique for quantifying transport in microchannels.

Evanescent-wave particle velocimetry was therefore used by Ph.D. student Necmettin Cevheri to study near-wall particle dynamics of a = 125 nm and 245 nm PS particles in combined EO and Poiseuille flow. The major research findings of this work are:

I. The changes in the average wall-normal positions of the a = 245 nm particles due to dielectrophoretic-like repulsion and (much weaker) shear-induced electrokinetic lift increase the average velocity sampled by the tracers
II. Unexpectedly strong repulsion is observed in combined EO and Poiseuille flow, and initial estimates of the magnitude of this repulsive force suggest that "the whole is

greater than the sum of the parts"—in other words, the magnitude of this force it is greater than the sum of the dielectrophoretic-like repulsion and shear-induced electrokinetic lift force magnitudes.

These results are detailed next, and have been presented at two national and international conferences:

1) Cevheri, N. and Yoda, M. "Nonlinear electrokinetic repulsion effects in combined electroosmotic and Poiseuille flow through microchannels," 65th Annual Meeting of the American Physical Society Division of Fluid Dynamics, San Diego, CA (2012)
2) Cevheri, N. and Yoda, M. "Evanescent-wave particle velocimetry studies of combined electroosmotic and Poiseuille flow," 10th International Symposium on Particle Image Velocimetry (PIV13), Delft, the Netherlands (2013)

The results in conference paper (item 2) will be submitted to *Langmuir* by the end of this calendar year. In addition, a paper summarizing the results from year two of this grant on how divalent cations affect EO flow and wall zeta-potentials was published in early 2013:

3) Cevheri, N. and Yoda, M. (2013) "Evanescent-wave particle velocimetry measurements of zeta-potentials in fused-silica microchannels," *Electrophoresis* **34**, 1950−1956

Copies of this paper, as well as the conference paper (item 2) are available at https://extranet.aro.army.mil/progress-reports.

Experimental Studies

Experimental Details

Electroosmotic and Poiseuille flows were studied in wet-etched fused-silica microchannels with trapezoidal cross-sections of depth ~30 μm and width ~300 μm driven by electric fields $\vec{\mathbf{E}} = E\hat{\mathbf{i}}$ (where E < 33 V/cm and $\hat{\mathbf{i}}$ is along the direction of the Poiseuille flow) and pressure gradients $\Delta p/L$ < 1.1 Bar/m, corresponding to a simple shear flow with a shear rate $\dot{\gamma} < 1600$ s^{-1}. Joule heating effects were minimal; in all cases, the temperature of the fluid, measured by a thermocouple at the exit in some of the experiments, was within 1 °C of the ambient temperature, which varied from 19 °C to 21 °C.

The working fluid was a degassed 1 mM aqueous sodium tetraborate ($Na_2B_4O_7$) seeded with fluorescent carboxylate-terminated polystyrene (PS) particles of radii a = 125 nm with a manufacturer-quoted polydispersity of 4.5 nm (Invitrogen F8811) or a = 245 ± 7.5 nm (Invitrogen F8812). The bulk particle number density of the working fluid c_∞ = 2.7×10^{16} m^{-3}, corresponding to volume fractions of 2.2×10^{-4} and 1.7×10^{-3} for the a = 125 nm and a = 245 nm particles, respectively.

The microchannel was mounted on the stage of an inverted epi-fluorescence microscope (Leica DMIRE2) and illuminated with evanescent waves generated at the bottom surface of the microchannel from the total internal reflection (TIR) of an argon-ion laser beam coupled into the substrate with prism. The intensity-based penetration depth of

the evanescent wave z_p = 110 nm–120 nm. Pairs of particle exposures with an exposure time τ = 0.5 ms with a spacing within the pair Δt = 2 ms and a spacing between pairs of 200 ms were generated using an acousto-optic modulator (AOM) "shutter" the laser; a sequence of 500 image pairs (= 1000 images) were recorded for a total data acquisition time of about 100 s. The fluorescent particles suspended in the flow in the center of the microchannel (to minimize any effect of side walls) were imaged through a 63× microscope objective onto an electron multiplying charge-coupled device (EMCCD) camera to give images of the flow over a region with dimensions of 130 μm × 37 μm.
After identifying and removing the images of overlapping or aggregated tracers, the displacements of the remaining particles in the plane parallel to the wall were determined by matching particles between the two images in the pair to their nearest neighbor. The particle-wall separation h, or the distance between the particle edge and the wall, was next determined from the particle image intensity I_p, the area-averaged integral of the grayscale values in the image. Assuming that the particle image intensity has the same exponential decay as the illumination

$$I_p(h) = I_p^0 \exp\left\{-\frac{h}{z_p}\right\} \tag{2}$$

The ensemble of particle-wall separations for about 3×10^4 particle images was then used to calculate the particle number density profile $c(h)$ over bins with a width (dimension normal to the wall) of 20 nm.

The particle displacements were divided into three layers, each containing a similar number of particle samples, based on h:

I. $0 \le h \le 100$ nm
II. 100 nm $\le h \le$ 200 nm
III. 200 nm $\le h \le$ 300 nm

and the particle velocity components parallel to the wall were then simply the particle displacement divided by Δt.

Results and Discussion

Figure 2 shows the flow velocity profiles $U(z)$ for Poiseuille flow (with no electric field) on the left at pressure gradients $\Delta p/L$ = 0.43 Bar/m (*circles*), 0.74 Bar/m (*triangles*), and 1.04 Bar/m (*squares*) estimated from a = 125 nm (*open symbols*) and a = 245 nm (*filled symbols*) particles for $z \le$ 540 nm, and for combined EO and Poiseuille flow at the same pressure gradient values and E = 8.8 V/cm. For Poiseuille flow, the data are consistently higher than the velocity profile predicted by the analytical solution (solid lines); we suspects that the discrepancy may be due to calibration errors, specifically in determining I_p^0 (*cf.* Eq. 2) since the slope of the data are in good agreement with the predicted shear rate and that the data for both particle sizes are in good agreement. As expected, the EO flow creates an "offset" in the flow velocity (proportional to E, over the

range of electric fields studied here, though results are not shown here), and the slope of the data are in good agreement with that of the Poiseuille flow (dashed lines).

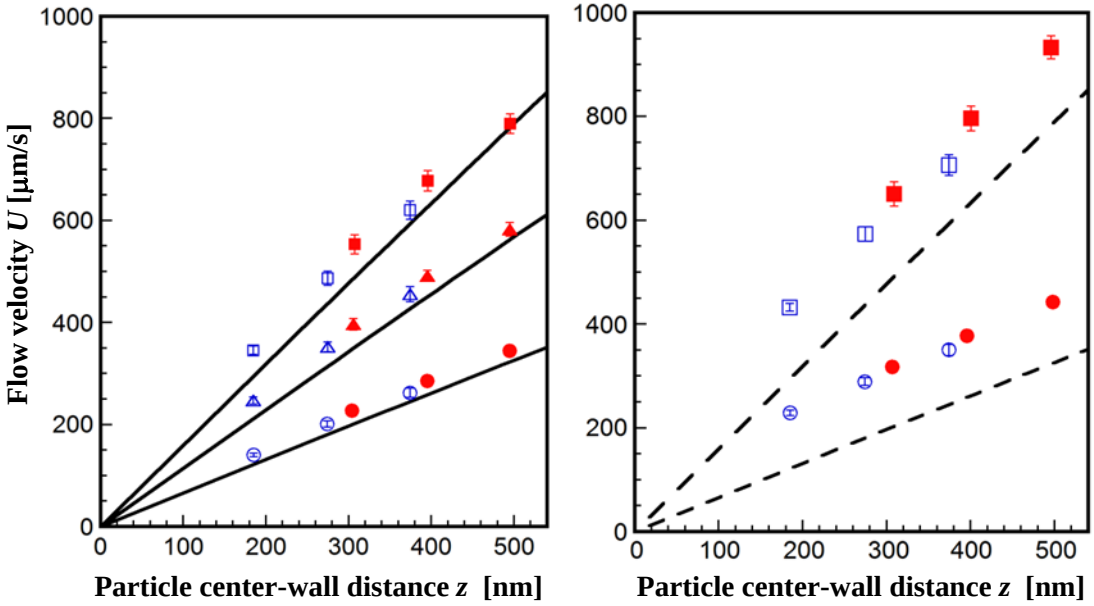

Figure 2 Flow velocity profiles for Poiseuille flow ($E = 0$) at $\Delta p/L$ = 0.43 Bar/m (*circles*) and 1.04 Bar/m (*squares*) [left] and combined Poiseuille and EO flow [right] at E = 8.8 V/cm measured by a = 125 nm (*open*) and a = 245 nm (*filled symbols*) particles. The dashed lines represent the analytical solution for Poiseuille flow at the same values of $\Delta p/L$. The error bars denote the standard deviations over three independent experiments. Both graphs have the same vertical axis label.

The distribution of such colloidal particles near the wall will be nonuniform because electrostatic repulsion due to particle-wall EDL interactions mediated by attractive van der Waals forces due to permanent and induced dipole interactions [13], as described by the classic Derjaguin-Landau-Verwey-Overbeek (DLVO) theory of colloid science [3]. If one were to assume instead that the particles are uniformly distributed over particle-wall separations $0 \le h \le 300$ nm, the average velocity sampled by the particles in this simple shear flow should be the flow velocity at the average z-position of the particle center of $\overline{z}_c = a + 150$ nm. Table I compares the average velocities obtained with the particles of different sizes with the expected value of the velocity at $\overline{z}_c$ for the combined EO and Poiseuille flow case shown in Fig. 1 on the right. Although particles of different a of course have different velocities in this simple shear flow due to excluded volume effects, the results for $\Delta p/L$ = 1.04 Bar/m demonstrate that particles of different sizes can measure different velocities in the same flow—here, the velocities measured by the a = 125 nm particles are in reasonable agreement with the expected values, while those measured by the larger a = 245 nm particles are not because these particles experience much stronger repulsion forces, that are discussed next.

Shear-induced electrokinetic lift and the dielectrophoretic-like repulsion were quantified in terms of near-wall particle distributions, expressed in terms of the particle

Table I. Comparison of average and expected velocities in combined flow at E = 8.8 V/cm measured by particles of different radii.

$\Delta p/L$ [Bar/m]	a = 125 nm		a = 245 nm	
	Avg. velocity [μm/s]	Exp. velocity at $\bar{z}_c$ = 275 nm [μm/s]	Avg. velocity [μm/s]	Exp. velocity at $\bar{z}_c$ = 395 nm [μm/s]
0.43	250	270	360	350
1.04	530	520	810	690

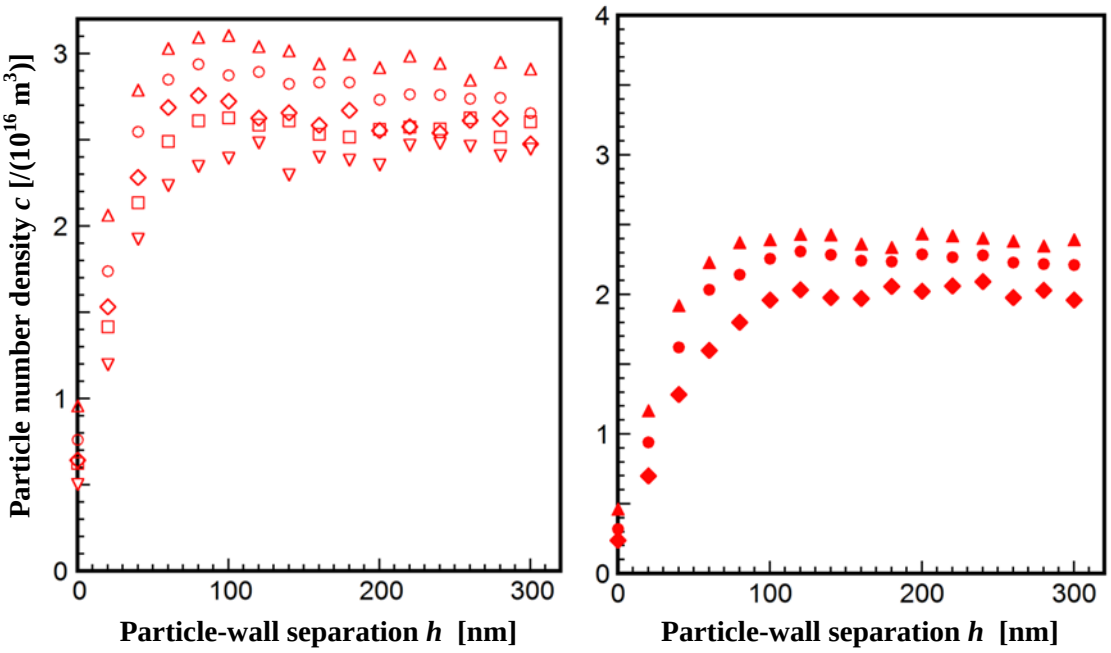

Figure 3 Particle number density profiles $c(h)$ for EO flow ($\Delta p/L \approx 0$) at E = 0 (△), 2.4 (○), 4.7 (◇), 7.1 (□) and 8.8 V/cm (▽) [left] and for Poiseuille flow (E = 0) at $\Delta p/L$ = 0.43 (▲), 0.74 (●) and 1.04 Bar/m (◆). In both cases, the bulk particle number density $c_\infty = 2.7\times10^{16}$ m^{-3}. Both graphs have the same vertical axis label.

number density c as a function of the particle edge-wall separation h. Figure 3 shows $c(h)$ for the a = 245 nm particles in EO flow (with $\Delta p/L \approx 0$) at E = 0 V/cm (△), 2.4 V/cm (○), 4.7 V/cm (◇), 7.1 V/cm (□) and 8.8 V/cm (▽) on the left, and in Poiseuille flow (with E = 0) at $\Delta p/L$ = 0.43 Bar/m (▲), 0.74 Bar/m (●) and 1.04 Bar/m (◆). For the "baseline" EO flow case of E = 0 (which is a very weak Poiseuille flow) c first increases with h, reaching a maximum value at $h \approx 100$ nm, then decreases slightly to a value comparable to the particle number density in the bulk fluid $c_\infty = 2.7\times10^{16}$ m^{-3}. The number density then decrease at a given h as E increases in the EO flow cases on the left, consistent with our previous observations of the dielectrophoretic-like repulsion force. Similarly, c decreases slightly at a given value of h as $\Delta p/L$ increases in the Poiseuille flow

cases on the right, due to shear-induced electrokinetic lift. No such effects were observed for the smaller a = 125 nm particles.

Figure 4 shows $c(h)$ for combined EO and Poiseuille flow at $\Delta p/L$ = 0.43 Bar/m on the left and $\Delta p/L$ = 1.04 Bar/m on the right, both also at E = 0 V/cm (△), 2.4 V/cm (○), 4.7 V/cm (◇),7.1 V/cm (□), and 8.8 V/cm (▽). A comparison of these number density profiles with the case of negligible shear shown in Figure 3 [left] shows that the decrease in the number of near-wall particles with E is surprisingly large for these combined flow cases, with c values an order of magnitude less than c_∞ for $E \geq 7.1$ V/cm. This marked decrease also appears to increase with $\Delta p/L$. Indeed, almost no particles were observed at $h \leq 300$ nm at $E > 8.8$ V/cm, which is why no cases are shown at larger E. This marked decrease in the number of near-wall particles, and the resultant increase in the average z-position of the tracers, is consistent with the average velocity sampled by these particles being significantly larger than the expected value at $\Delta p/L$ = 1.04 Bar/m in Table I.

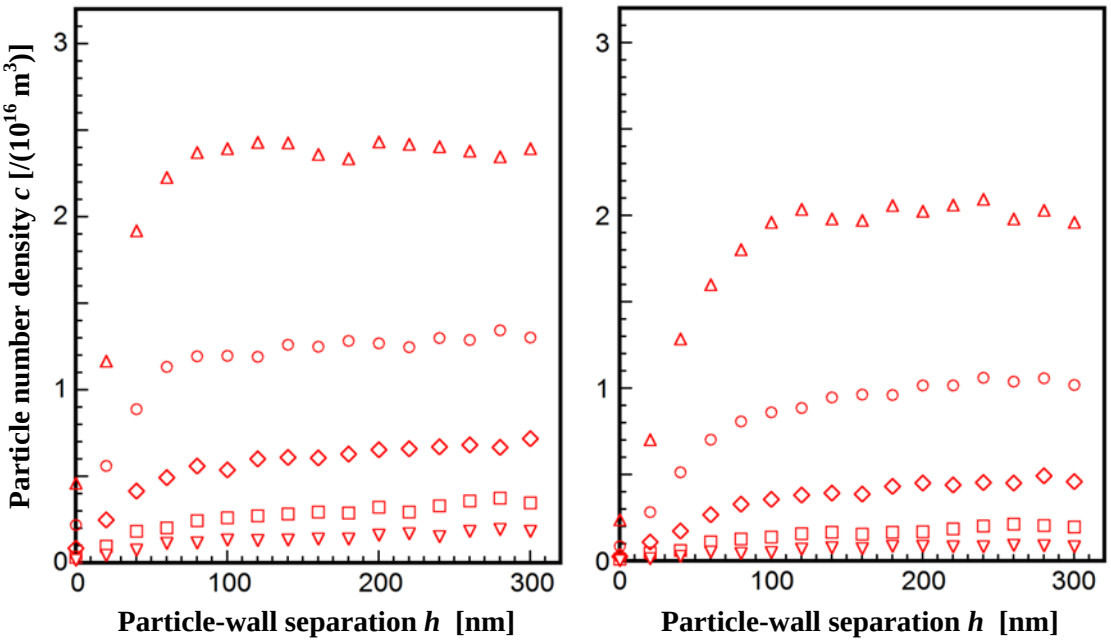

Figure 4 Particle number density profiles $c(h)$ for combined EO and Poiseuille flow ($\Delta p/L \approx 0$) at E = 0 (△), 2.4 (○), 4.7 (◇), 7.1 (□) and 8.8 V/cm (▽) and $\Delta p/L$ = 0.43 Bar/m [left] and for the same range of E values and $\Delta p/L$ = 1.04 Bar/m.

This large decrease also suggests that the force driving these particles away from the wall likely exceeds the sum of the dielectrophoretic-like repulsive and shear-induced electrokinetic lift forces. The magnitude of this force was hence determined from the slope of the potential energy profile $\phi(h)$ of the particle-wall interaction, which can be estimated from these measured $c(h)$ assuming that they follow a Boltzmann distribution. To try to isolate the effect of the electric field (from that of the pressure gradient), the potential energy for the case of "only" Poiseuille flow (*i.e.*, when E = 0) was subtracted

from that combined Poiseuille and EO flow at the same $\Delta p/L$. Table 2 compares the magnitude of the resultant "additional" repulsive force $\overline{F}_C^E$ (averaged over 80 nm ≤ h ≤ 280 nm) which should be due "only" to E, was compared with the magnitude of the dielectrophoretic-like repulsive force $\overline{F}_{EO}$ estimated from the cases shown in Figure 3 [left] of EOF (with $\Delta p/L \approx 0$) at the same value of E. The results clearly show that the additional repulsive force $\overline{F}_C^E$ is much greater than the corresponding value of $\overline{F}_{EO}$ observed in the absence of the flow shear due to Poiseuille flow. The uncertainty in these force estimates is quite large, about 3 fN based on the results of three independent experiments, but the differences between $\overline{F}_C^E$ and $\overline{F}_{EO}$ are greater than the uncertainty for $E \geq 4.7$ V/cm. These results in combined EO and Poiseuille flow therefore show that there is creates a strong wall-normal force:

- that repels negatively charged dielectric particles suspended in a conducting medium with mobile electrolytes from the surface of a negatively charged wall
- with a magnitude that is significantly greater than the sum of the dielectrophoretic-like repulsive force observed in EO flow and the shear-induced electrokinetic lift force observed in Poiseuille flow

suggesting that there is a nonlinear interaction between the electric field and flow shear.

Table II Estimates of the forces due to the presence of an electric field in "pure" EOF and in combined EO and Poiseuille flow. The uncertainty in these force estimates is about 3 fN, and the estimates for $\overline{F}_{EO}$ at the two lowest values of E are less than 0.1 fN.

E [V/cm]	$\overline{F}_{EO}$ [fN]	$\overline{F}_C^E$ [fN] $\Delta p/L = 0.43$ Bar/m	$\overline{F}_C^E$ [fN] $\Delta p/L =$ 1.04 Bar/m
2.4	0	2.0	3.5
4.7	0	5.1	5.4
7.1	1.2	8.3	8.9
8.8	2.1	9.2	14.2

Theoretical/Computational Results and Research Accomplishments

As a first step of the project, we reviewed the fundamental theory of the motion of a collection of colloidal particles near solid walls and to compare theoretical computations with the experiments conducted by Kazoe and Yoda [4] for electroosmotic flow. Understanding the near-wall transport of suspended particles is also relevant to a number of microfluidic applications where a two- or three-dimensional array of colloidal particles is assembled on a solid substrate. We predicted the velocity of a single colloidal particle using Henry's Law of electrophoresis and found that the presence of the wall does not appreciably affect the convection velocity. In Year 2 we developed methods of describing the motion of single colloidal particles and subsequently show an approach to describe the motion and distribution of a collection of particles (a mass transfer approach) where the particles are considered to be the third species in an electrolyte mixture. The parameter range of interest in the experiments was identified and the results for the particle velocity were compared with the results of a single-particle electrophoresis study. The particle distribution is obtained using the aforementioned mass transfer approach and the results for both the velocity and the particle distribution compare well with the experimental results. Surprisingly, the presence of the walls has little or no effect on the particle velocity. When the electrostatic lift force on the particles was identified, a review of the principles and fundamentals of DLVO and non-DLVO surface forces was performed.

In order to analyze the corresponding influence of DLVO and non-DLVO forces on the interaction of the channel wall and a single colloidal particle, in Year 3 we performed molecular dynamics simulations. The results of molecular dynamics will be compared against a continuum DLVO approach. A future objective of this study is to develop a unified theory of the motion of a distribution of colloidal particles near walls. We speculate that the reason the particle velocity is independent of the distance from the surface as shown in Year 2 work is because the electrostatic repulsive forces (EDL repulsion) keep the particles far enough away from the channel walls that surface effects do not affect the particle motion.

The force between molecules can be purely physical in nature or they may involve chemical association. The van der Waals interaction should be distinguished from the chemical one which brings about molecule formation therefore the origin of van der Waals forces is purely physical. In fact, van der Waals forces are of electrostatic nature, universal (acting on charged or neutral molecules) and non-local. They act between all the molecules and macroscopic bodies. Van der Waal forces between the molecules depend on the polarizability of the molecules, i.e. on the extent of the possible charge displacements inside the molecule or atoms as molecules are not rigid entities.

The electrostatic force between surfaces can be attractive or repulsive; it depends on the surface charge density and surface potential of each surface, and the physical

properties of the medium separating the two surfaces. When surfaces are immersed in water, the high dielectric constant of the water causes surface groups to dissociate, which results in a charged interface. Furthermore selective adsorption of ions from an electrolyte solution can charge a surface.

An example of this is the dissociation of silanol groups at the surface of a silica substrate. The dissociation of the surface silanol groups creates a diffuse layer of oppositely charged ions, whose concentration decreases as a double exponential with distance away from the solid-liquid interface. When double layers from opposing surfaces of equal charge overlap, a repulsive force results between the two surfaces.

The major research findings of the theoretical/computational work are:

1) The velocity of a single colloidal particle using Henry's Law of electrophoresis and found that the presence of the wall does not appreciably affect the convection velocity;
2) Using a mass transfer approach, the concentration of the colloidal particles near the wall is qualitatively similar to the experimental results;
3) The largest near-wall force between a colloidal particle and a charged wall is likely the long-range electrostatic force.
4) Using molecular dynamics methods, the effect of divalent ions is tpo increase the bulk velocity in nanochannels.

In the last 12 months, the project has produced one ISI journal article [25] already published and two papers in preparation. One abstract for oral presentation at the annual meeting of the Division of Fluid Dynamics (DFD) of the American Physical Society (APS) 2012 and at the 51st AIAA Aerospace Sciences Meeting 2013. The title of the abstract and paper is ``Effect of divalent ions on electroosmotic transport in a sodium chloride aqueous solution confined in an amorphous silica nanochannel'' by Harvey Zambrano and A, T, Conlisk. The AIAA paper will be submitted to an archival journal soon.

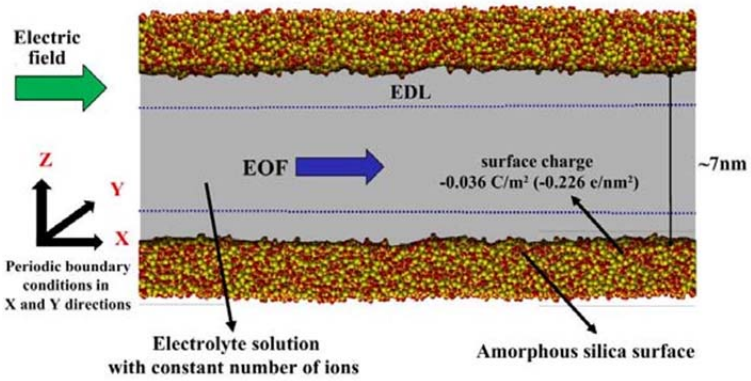

Silica slabs: 34.76nm x 2.87nm x ~3.10 nm
Water molecules: 20500
Ions: 170 ions (NaCl ions + divalent ions 6, 18 and 31%)
Computational box: 34.76 x 2.87 x 30nm

Figure 5 Schematic of the system. The sketch shows the geometric specifications of the simulated system for the MD study of the effect of divalent ions.

Simulation Details

Since details of the simulations in Year 1 and Year 2 are available in previous reports, we describe here only the details of the divalent ion computations.

Molecular simulations with different degrees of complexity, have been successfully conducted to study electrokinetic transport in interfaces, nanochannels, nanopores, and carbon nanotubes [16]. In this study, we perform Molecular Dynamics simulations. We use the MD package FASTTUBE. This package has been used to study several nanofluidic systems including water in and around carbon nanotubes, electroosmotic flows on silica substrate and capillary flow in silica nanochannels. In this work, we simulate a silica nanochannel as shown in Figure 5. The channel has dimensions of 34.76 nm in X direction, 2.53 nm in Y direction and 7 nm in Z direction, being periodic in X and Y directions. The computational box is 26 nm long in Z direction in order to avoid interactions with periodic images in that direction. A SPME algorithm with slab correction is implemented to compute the long-range electrostatic interactions.

In order to equilibrate the electrolyte solution, MD simulations are performed during 2.0 ns using a time step of 2 fs. During the simulations silica is kept frozen. Calibrating the interaction potential to match the experimental value of the water contact angle removes the observation of ice [17]. The system is coupled to a Berendsen thermostat at 300 K during the first 0.5 ns which is disconnected for the rest of the simulation. Subsequently, axial electric fields are applied to the systems and NEMD simulations are conducted with a time step of 2 fs until the properties (density and electroosmotic velocity) in the bulk region are not changing, during this set of simulations the system is connected again to a Berensend thermostat with a time constant of 0.1 ps to keep the temperature at 300 K. We run similar simulations for NaCl aqueous solutions with different amounts of divalent ions, corresponding to 6, 18 and 30% of the total amount of ions disolved in the solution. In all the simulations, we keep electroneutrality in the systems by fixing the ionic strength of the electrolyte solution. Constant electric fields between 0.2 V/nm and 1.0 V/nm are applied to the system in parallel direction to the walls. The large electric fields applied in this study are needed to enhance signal-to-noise ratio from simulations. Nevertheless, the values of the applied electric fields are in line with previous MD simulations of EOF in nanochannels [18] and with some experimental studies.

An aqueous solution of sodium chloride consisting of 20500 water molecules and 170 ions is confined in a amorphous silica channel with surface charge density of 0.227 e nm^{-2}. A corresponding Debye length of 0.65 nm is computed.

More than 28 cases with different configurations are studied (two divalent ionic species and 4 different electric fields applied to each case). For each case a set of simulations is run during more than 40 ns extracting data from the last 10 ns. During

the production run, the temperature of the water will be permanently computed to confirm the temperature of the system is kept constant.

Results and Discussion

Mass Transport Model of the Particle Distribution

In this view, the colloidal particles are treated simply as an additional species characterized by its concentration within the electrolyte buffer. The governing equations for this process are the unsteady Navier-Stokes equations along with continuity and the Poisson-Nernst-Planck system for the electro- static part of the problem.

In experimental studies, particles are generally assumed to follow the bulk fluid motion; however, it is seen here that if the particles are charged they will deviate from the bulk fluid motion by the magnitude of the electromigration term, the particles will also deviate from the mean bulk fluid motion if diffusion is important. However this term is usually small. This method of modeling the motion of particles has led to acceptable agreement with experiments[17].

Because of the presence of the bounding walls in a direction normal to the walls of the channel the net flux of particles and ions as well as the solvent will be zero. Thus each of the charged species will have concentrations that follow the Boltzman distribution.

The polystyrene particles are assumed to have a valence z_p that is much greater that the ionic species, and the potential is calculated numerically for a variety of valences for the parameters of Kazoe and Yoda [4]. The results for the particle number distributions are shown on Figure 6. Note that the computational results for large valence show a displacement from the wall due to the large negative value of the particle valence. This of course is rather artificial since for such a large valence steric effects may arise that are not included here. Nevertheless, the simple model for the number density agrees qualitatively with the results from the experiments.

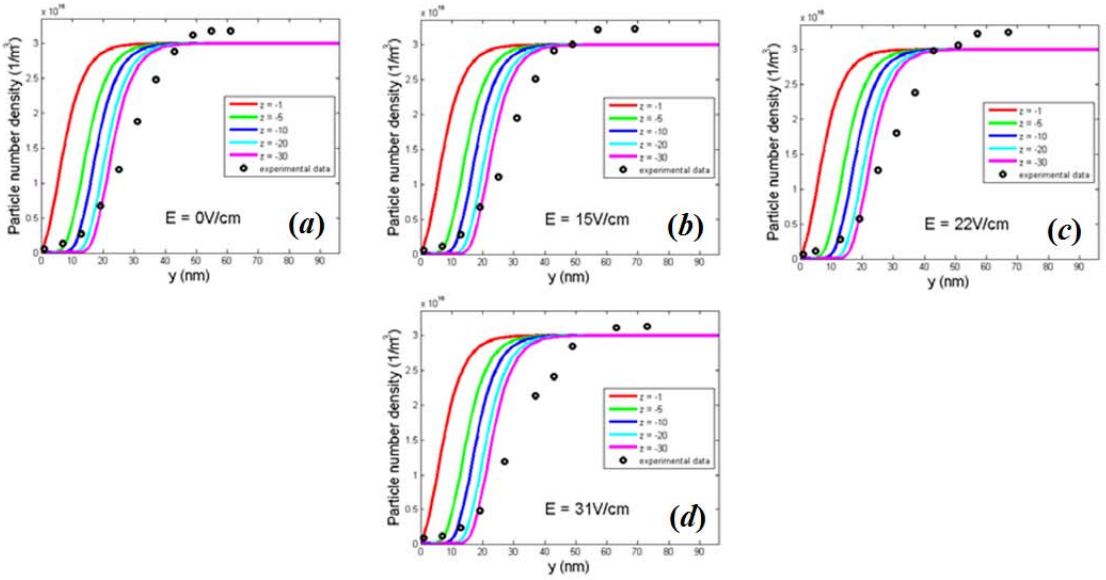

Figure 6 Particle number density in EOF as a function of the distance between the wall and the particle edge at applied electric fields of *a*) 0 V/cm; *b*) 15 V/cm; *c*) 22 V/cm and *d*) 31 V/cm. The different line colors represent different particle valences.

Effect of Divalent Ions

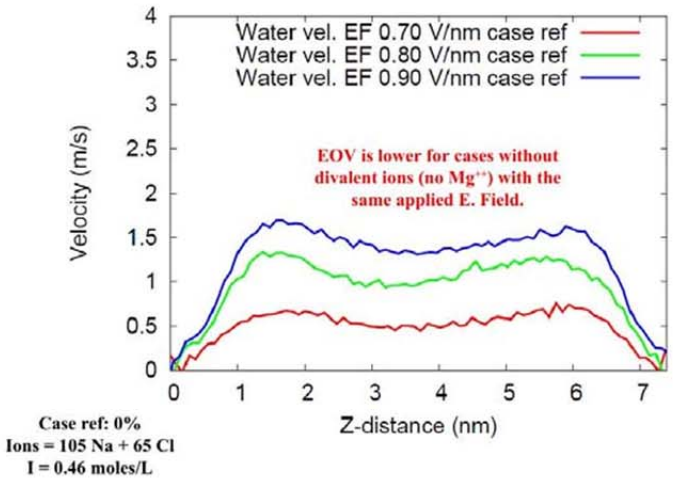

Figure 7 Water velocity profiles for a solution of sodium and chloride confined in a silica nanochannel. Linear response can be verified with these profiles as different electric field are applied parallel to the channel walls.

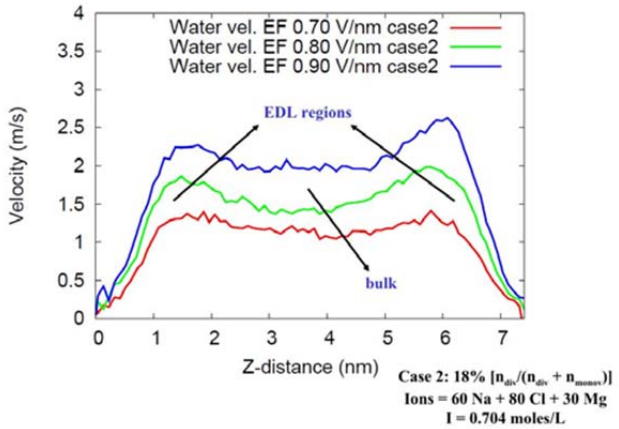

Figure 8. Water velocity profiles for a solution of magnesium, sodium and chloride confined in a silica nanochannel. The concentration of calcium correspond to the 18% of the total of the salt present in the electrolyte solution. Linear response can be verified with these profiles as different electric field are applied parallel to the channel walls.

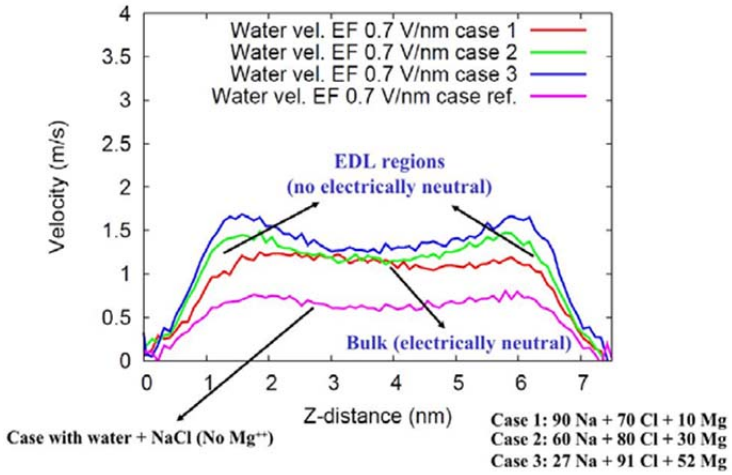

Figure 9 Water velocity profiles for a solution of magnesium, sodium and chloride confined in a silica nanochannel as a electric field of 0.7 V/nm is applied parallel to the channel walls. The concentration of magnesium varies for each case from 0% to 31% of the total of the ions present in the electrolyte solution. Higher concentrations of magnesium result in an electroosmotic velocity increase at the Electric Double Layer (EDL).

We compute the density and velocity profiles by using the binning method with a binning size of 0.12 nm. Simulations were conducted during 55 ns and results have been extracted from the last 35 ns of the simulation. Linear response of the system can be inferred from Figures 8 and 9 that depict the velocity profile averaged over the simulation length. Comparing Figure 7 (no Mg^{++}) with Figure 5 (with Mg^{++}), the velocity is considerably higher in contrast to the experimental results as described above in Figure 1. Moreover, Figures 8 and 9 show that the velocity increases as the concentration of the divalent ion increases. Figure 9 shows that the counter-ions (Na^{+} and Mg^{++}) are attracted near the negatively charged silica walls while the co-ions Cl^{-} are repelled to the bulk fluid. However, Mg^{++} ions are farther away from the walls in comparison to Na^{+} ions, likely due to the stronger Mg^{++} affinity for water. In fact, we

compute binding energies of −425 kJ mol^{-1} for the interaction between Na^{+} ions and water, and of −510 kJ mol^{-1} for the interaction between Mg^{++} ions and water. The computed binding energies confirm that Mg^{++} ions have a higher affinity for water than Na^{+} ions which results in a more robust hydration in line with the results found by Calero *et al.* [18].

These results show that Mg^{++} is much more effective dragging water molecules due to its hydration layer being much more robust so the electroosmotic velocity increases where the proportion of Mg^{++} is higher In the bulk the local electroneutrality prevents changes in the electroosmotic velocity in this area due to the proportion of co-ions and counter-ions keep the same for different cases and different applied axial electric fields. The results suggest that by varying the proportion of divalent ions in a multivalent electrolyte solution under nanoconfinement, it is possible to exert control on the electroosmotic velocity near the channel walls.

Summary

These surprising results suggest that the effect of combined EO and Poiseuille flow on colloidal particle dynamics are quite complex, even though the fluid velocity fields for these creeping flows superpose. Although this project is over, Dr. Yoda's group is still studying particle dynamics in combined EO and Poiseuille flow, at present mainly for $E < 0$ (*i.e.*, when the EO and Poiseuille flows are in opposite directions supported by a grant from the National Science Foundation. Dr. Conlisk will continue work on modeling and simulation of these transport processes.

References

[1] Reyes, D. R., Iossifidis, D., Auroux, P.-A., and Manz, A. (2002) Micro Total Analysis Systems. I. Introduction, Theory and Terminology, *Analytical Chemistry* **74**, 2623

[2] Ohno K., Tachikawa, K., and Manz, A. (2008) Microfluidics: Applications for Analytical Purposes in Chemistry and Biochemistry, *Electrophoresis* **29**, 4443

[3] Probstein, R. F. (2003) *Physicochemical Hydrodynamics: An Introduction* (2nd ed.). Wiley (Hoboken, NJ)

[4] Kazoe, Y. and Yoda, M. (2011) An experimental study of the effect of external electric fields on interfacial dynamics of colloidal particles. *Langmuir* **27**, 11481

[5] Pouya, S., Koochesfahani, M., Snee, P., Bawendi, M. and Nocera, D. (2005) Single quantum dot (QD) imaging of fluid flow near surfaces. *Experiments in Fluids* **39**, 784

[6] Huang, P., Guasto, J. S. and Breuer, K. S. (2006) Direct measurement of slip velocities using three-dimensional total internal reflection velocimetry. *Journal of Fluid Mechanics* **566,** 447

[7] Bouzigues, C. I., Tabeling, P. and Bocquet, L. (2008) Nanofluidics in the Debye layer at hydrophilic and hydrophobic surfaces. *Physical Review Letters* **101**, 114503

[8] Yoda, M. and Kazoe, Y. (2011) Dynamics of suspended colloidal particles near a wall: Implications for interfacial particle velocimetry. *Physics of Fluids* **23**, 111301

[9] Wereley, S. T. and Meinhart, C. D. (2010) Recent advances in micro-particle image velocimetry. *Annual Review of Fluid Mechanics* **42**, 557

[10] Bike, S. G., Lazarro, L. and Prieve, D. C. (1995) Electrokinetic lift of a sphere moving in slow shear flow parallel to a wall: I. Experiment. *Journal of Colloid and Interface Science* **175**, 411

[11] Yariv, E. (2006) Force-free electrophoresis? *Physics of Fluids* **18**, 031702

[12] Schnitzer, O., Frankel, I. and Yariv, E. (2012) Shear-induced electrokinetic lift at large Péclet numbers. *Mathematical Modelling of Natural Phenomena* **7**, 64

[13] Bevan, M. A. and Prieve, D. C. (1999) Direct measurement of retarded van der Waals attraction. *Langmuir* **15**, 7925

[14] Werder, T., Walther, J.H., Jaffe, R. L., Halicioglu, T., and Koumoutsakos, P. (2003) On the water- graphite interaction for use in MD simulations of graphite and carbon nanotubes, *J. Phys. Chem. B*, **107**, 1345.

[15] Ho, C., Qiao, R., Heng, J. B., Chatterjee, A., Timp, R. J., Aluru, N. R. and Timp, G. (2005) Electrolytic transport through a synthetic nanometer-diameter pore, *Proc. Natl. Acad. Sci. USA*, **102**, no. 30, 10445.

[16] Prakash, S., Piruska, A., Gatimu, E. N., Bohn, P. W., Sweedler, J. V., and Shannon, M. A. (2008) Nanofluidics: Systems and applications, *IEEE Sens. Journal*, **8**, no. 5, 441.

[17] Attard, P. and Batchelor, M. T. (1988) A mechanism for the hydration force demonstrated in a model system, *Chem. Phys. Lett.*, **149**, no. 2, 206.

[18] Calero, C., Faraudo, J., and Aguilella-Arzo, M., (2011) Molecular Dynamics simulations of concentrated aqueous electrolyte solutions, *Mol. Sim.*, **37**, No. 2, 2011, 123.